


Analysis of Biodistribution and in vivo Toxicity of Varying Sized Polystyrene Micro and Nanoplastics in Mice

Bohai Du¹, Tianlan Li¹, Haoqi He¹, Xun Xu², Chunmei Zhang¹, Xianzhu Lu¹, Yuhan Wang¹, Jingyi Cao¹, Yinghan Lu¹, Yiwa Liu¹, Shanshan Hu¹, Juxiao Li¹, Li Li¹ , Ming Shi¹

¹Dongguan Key Laboratory of Environmental Medicine, School of Public Health, Guangdong Medical University, Dongguan, Guangdong Province, 523808, People's Republic of China; ²Experimental Animal Center, Guangdong Medical University, Dongguan, Guangdong Province, 523808, People's Republic of China

Correspondence: Li Li; Ming Shi, School of Public Health, Guangdong Medical University, Dongguan, Guangdong Province, 523808, People's Republic of China, Tel +86-15889530426; +86-769-22896568, Email lily2017@gdmu.edu.cn; shiming@gdmu.edu.cn

Introduction: Studies have shown that microplastics (MPs) and nanoplastics (NPs) could accumulate in the human body and pose a potential threat to human health. The purpose of this study is to evaluate the biodistribution and toxicity of MPs/NPs with different particle sizes comprehensively and thoroughly.

Methods: The purpose of this study was to investigate the biodistribution and in vivo toxicity of polystyrene (PS) MPs/NPs with different sizes (50 nm, 100 nm, and 500 nm). The BALB/c mice were given 100 μ L of PS50, PS100 and PS500 at the dosage of 1 mg/kg BW or 10 mg/kg BW, respectively, by gavage once a day. After 28 consecutive days of treatment, the biodistribution of differently sized PS MPs/NPs was determined through cryosection fluorescence microscopy and fluorescent microplate reader analysis, and the subsequent effects of differently sized PS MPs/NPs on histopathology, hematology and blood biochemistry were also evaluated.

Results: The results showed that the three different sizes of PS MPs/NPs were distributed in the organs of mice, mainly in the liver, spleen, and intestine. At the same time, the smaller the particle size, the more they accumulate in the body and more easily penetrate the tissue. During the whole observation period, no abnormal behavior and weight change were observed. The results of H&E staining showed that no severe histopathological abnormalities were observed in the main organs in the low-dose exposure group, while. Exposure of three sizes of PS MPs/NPs could cause some changes in hematological parameters or biochemical parameters related to heart, liver, and kidney function; meanwhile, there were size- and dose-dependencies.

Conclusion: The biological distribution and toxicity of plastic particles in mice were more obvious with the decrease of particle size and the increase of concentration of plastic particles. Compared with MPs, NPs were easier to enter the tissues and produce changes in liver, kidney, and heart functions. Therefore, more attention should be paid to the toxicity of NPs.

Keywords: microplastics, nanoplastics, polystyrene, size, biodistribution, nanotoxicology

Introduction

Plastic has become an indispensable material worldwide with a wide range of applications. It is predicted that approximately 12 billion tons of plastic will be released into the natural environment by 2050.¹ Most waste plastics are incinerated or buried in landfills, and then continuously fragmented into microplastics (MPs, with a diameter less than 5 mm) and nanoplastics (NPs, with a diameter less than 0.1 μ m) through weathering, ultraviolet radiation, external damage, or biodegradation, ultimately causing serious pollution to the global environment.²⁻⁴ Currently, MPs have been found in soil, water, air, and even in remote areas of the Arctic and Antarctica.⁵ Due to their excellent stability, small size and degradation resistance, MPs could accumulate in living organisms upon ingestion, and then enter the human body along with the food chain and food web, causing potential hazards to human health.^{6,7} In addition, some daily necessities and living habits of human beings may also cause direct contact and uptake of MPs and NPs. It is reported that MPs and NPs have been detected in human stool, placenta

and lung.^{8–10} Nevertheless, the knowledge of the potential biological effects following exposure to MPs and NPs in mammal and human remains remarkably limited.

Waste plastic particles may enter the human body through food, skin, and respiration. Recent studies have found that plastic packaging for drinking water and food is the main source of human contact with plastic particles.¹¹ Although MPs mainly enter human body through digestive tract, their absorption rate in the intestine is very low, and most of them are excreted through feces.¹² Yan et al detected plastic particles of different sizes and shapes in human feces and found that the fecal MP concentration in patients with inflammatory bowel disease was significantly higher than that in healthy individuals.¹³ Unlike MPs, NPs have smaller dimensions, larger specific surface area, and more active interactions with cell membranes. They are more likely to pass through various biological barriers and be transported by body fluids to various tissues and organs throughout the body, accumulating and causing functional impairments.^{14,15} PS is a widely used thermal insulation plastic, especially in disposable drinking cups, packaging bag, electronic products and personal care products.¹⁶ Kopatz et al orally administered polystyrene micro/nanoparticles (PS MPs/NPs) of different sizes (9.55 μm , 1.14 μm , 0.293 μm) to mice, and found that 0.293 μm PS particles could penetrate the blood–brain barrier and enter brain tissue only 2 hours after gavage, which may increase the risk of inflammation, neurological disorders, and neurodegenerative diseases.¹⁷

Analogous to most micro and nano materials, the size, composition, morphology, aging time, and surface properties of plastic particles are closely related to the adverse effects on organisms. Among them, particle size is the most important factor determining biological distribution and degree of damage of particles.¹⁸ It is generally believed that nanoparticles with smaller sizes and higher specific surface area may be more toxic to living organisms due to their strong biological penetration power. Zhou et al exposed white legged shrimp to water containing PS MPs four different sizes (0.1, 1.0, 5.0, or 20.0 μm) and found that the intake and excretion of PS MPs had a size-dependent effect, smaller particles were more bioavailable, and exhibited greater histopathological damage to the intestine and gills of the shrimp.¹⁹ Plastic particles ingested through the digestive tract will enter the circulatory system and distribute in various tissues and organs, and its distribution range is related to particle size.²⁰ When the particle diameter was less than 150 μm , it is likely to cross the intestinal mucosal barrier, and only particles with the diameter less than 1.5 μm can be transported to deeper tissues.^{21,22} When the particle size of plastic particles is less than 200 nm, it is easier to accumulate in liver, lung, spleen, kidney and other organs. However, nanoparticles smaller than 10 nm will be rapidly filtered by glomerulus and excreted with urine.^{23,24}

Previous studies have shown that MPs and NPs could accumulate in organisms and distribute in the liver, spleen, lung, blood, and testis.^{25,26} Meanwhile, with the decrease of particle size, the absorption and biological distribution of plastic particles in organisms increased.^{27,28} In addition, relevant studies have found that NPs can cause toxic effects on marine and freshwater species, including bacteria, including planarians, zebrafish and fathead minnows.^{29–31} However, current research on the toxicity of PS MPs/NPs mainly focuses on single sizes with different exposure doses or surface modifications, or using in vitro cell model or simple model organisms, which limits the prediction of potential toxicity of MPs and NPs to mammals, especially humans. Thus, it is crucial to investigate the distribution and potential toxicity of MPs/NPs with different particle sizes in mammalian models and to compare the differences of distribution and toxicity of different particle sizes in organisms.

In the present study, three different sizes of commercial PS particles with the same surface properties were selected to evaluate the in vivo distribution and biological toxicity. After 28 days of continuous gavage to mice, the distribution, behavior, body weight, organ coefficient, hematological parameters, serum biochemical parameters, and organ histopathology of the animal models in different-size PS MPs/NPs groups were detected and compared. Our research may provide a better understanding of the toxic effects of MPs/NPs at the mammalian level, and provide important insights into the potential risks of plastic particles of different sizes to human health.

Materials and Methods

Characterization of PS MPs/NPs

Three kinds of PS micro- and nanoplastics used in this study were purchased from Zhongke Leiming Company (Beijing, China). The sizes of the three PS particles were 50 nm (PS50), 100 nm (PS100), and 500 nm (PS500), respectively, and they had the same surface modification (carboxyl) and fluorescence spectra (emission wavelength: 660–680 nm). The size and morphology of the three sizes of PS MPs/NPs were confirmed by scanning electron microscope (SEM, MIRA

LMS, TESCAN, Czech Republic). The dispersion properties of the three sizes of PS MPs/NPs were analyzed by assessing the zeta-potential and hydrodynamic diameter using a dynamic light scattering (DLS) instrument (SZ-100, HORIBA, Japan).

Animals Care

A total of seventy healthy BALB/c mice (four weeks old) were purchased from Baishitong Animal Breeding Center (Zhuhai, China). The mice were raised in plastic cages with padding in a ventilated, temperature controlled and standardized sterile animal room, with 12 hours day/aperture. All animals were housed and acclimated the animal facility for 7 days prior to experimentation, and food and water were provided ad libitum. All operations in this study comply with the standards and requirements of the Experimental Animal Center of Guangdong Medical University and have been approved by the Animal Ethics Committee of Guangdong Medical University (Permit No. GDY2204042).

Animal Treatments and Sample Collection

Before intragastric administration, mice were randomly divided into 7 groups and three different particle sizes of PS MPs/NPs were prepared in different doses with ultrapure water. The specific grouping was as follows: (1) PS50 high-dose group (PS-50H), treated with 10 mg/kg BW (body weight) PS50; (2) PS50 low-dose group (PS50-L), treated with 1 mg/kg BW PS50; (3) PS100 high-dose group (PS100-H), treated with 10 mg/kg BW PS100; (4) PS100 low-dose group (PS100-L), treated with 1 mg/kg BW PS100; (5) PS high-dose group (PS500-H), treated with 10 mg/kg BW PS500; (6) PS500 low-dose group (PS500-L), treated with 1 mg/kg BW PS500; (7) Control group, treated with ultrapure water. The mice were given a volume of 100 μ L PS solution by gavage once a day for 28 consecutive days. The control group was orally given the same volume of ultrapure water. The survival status, food intake, fur, behavior, mental state, urine, feces, and weight of each mouse were recorded daily. After continuous gavage for 28 days, the mice were euthanized and dissected. Approximately 50 μ L of blood was collected into an anticoagulant tube for blood routine examination. The remaining blood was collected using a coagulation promoting tube and then centrifuged to obtain serum for blood biochemical analysis. The main organs (heart, liver, spleen, lung, kidney, brain, testis, intestine) were divided into three parts. Part of the tissue was fixed with 10% formalin for the evaluation of histopathological changes. Another part was embedded in optimal cutting temperature compound (OCT, Sakura Finetek, USA) for tissue fluorescence imaging. We immediately frozen the remaining tissue samples in liquid nitrogen and then stored them at -80°C .

Cryosection Fluorescence Microscopy

After 28 days of gavage treatment, the heart, liver, spleen, lung, kidney, brain, testis and intestine of each mouse were collected, embedded into OCT compound and frozen at -80°C . The tissue frozen section was cut into 5 μm thick by freezing microtome (CM3050S, Leica, Germany). The accumulation and distribution of PS in various tissues were observed by fluorescence microscope (BZ-X800LE, KEYENCE, Japan).

Quantification of Uptake in Organs

The liver, spleen, kidney, testis, and intestine of each mouse were cut and accurately weighed after draining the surface water. Take appropriate samples of organs and tissues, blot away excess surface moisture, and precisely weigh them. Based on the weight, tissue lysis solution (Beyotime) is introduced into the grinding apparatus to thoroughly disintegrate the organs and tissues. The fluorescent microplate reader (Infinite E Plex, TECAN, Switzerland) was utilized to detect the readings of each homogenate.

Histopathological Examination

Major organs of each mouse were fixed in 10% formalin. After gradient dehydration with different concentrations of alcohol in an automatic tissue dehydrator (APS300S, Leica, Germany), these tissues were embedded in paraffin blocks by paraffin embedding station (Leica, Germany), and then cut into 5- μm sections and stained by hematoxylin and eosin (H&E). The H&E staining of heart, liver, spleen, lung, kidney, brain, intestine, and testis was scanned by Digital Pathology Scanner (Aperio GT 450, Leica, Germany), and the histopathological changes were evaluated.

Hematology Analysis

Blood samples were collected from the posterior orbital venous plexus of mice after the mice were anaesthetized. About 50 μL blood was collected in pre-prepared tubes of heparin sodium, and then routine blood analysis was determined by a fully automated hematology analyzer (BC-2600Vet, Mindray Medical International Limited, China). These hematological indicators have been tested as follows, white blood cell (WBC) count, neutrophils (Neu) count, lymphocyte (Lym) count, red blood cell (RBC) count, hematocrit (HCT), mean corpuscular volume (MCV), hemoglobin concentration (HGB), mean corpuscular hemoglobin (MCH) and mean corpuscular hemoglobin concentration (MCHC), platelet (PLT) count, thromboplastin (PCT) and mean platelet volume (MPV).

Serum Biochemical Analysis

The whole blood of mice was collected in disposable venous blood vessels containing separating gel and the serum was obtained by centrifugation for 15 min at 4°C, 1150 g. The serum biochemical parameters were detected by automatic blood biochemical analyzer (BS-220, Mindray Medical International Limited, China). All matching reagents were purchased from Mindray Medical International Limited, China. The specific biochemical indexes in this study included alanine aminotransferase (ALT), aspartate transaminase (AST), alkaline phosphatase (ALP), total protein (TP), albumin (ALB), globulin (GLB), creatine kinase (CK), lactate dehydrogenase (LDH), triglyceride (TG), total cholesterol (TC), high-density lipoprotein (HDL-C), low-density lipoprotein (LDL-C), glucose (GLU), uric acid (UA), creatinine (CREA) and urea (UREA).

Statistical Analysis

All statistical analysis was performed with the SPSS25.0 statistical software and the figures were drawn with GraphPad Prism software package. Data were presented as mean \pm standard deviation (SD), and the statistical difference was analyzed by one-way analysis of variance (ANOVA). The results were considered statistically significant if $P < 0.05$.

Results

Characterization of PS MPs/NPs

SEM was used to observe the size, shape, and morphology of the three types of PS MPs/NPs. The representative images were shown in [Figure 1A–C](#). The three types of PS MPs/NPs were spherical shape with the diameter approximately 50, 100 and 500 nm. The hydrodynamic size distribution and zeta potential of these three sizes of PS MPs/NPs were also investigated and the results were shown in [Figure 1D–F](#). The hydrodynamic diameter of PS50, PS100 and PS500 was (83.10 ± 3.01) nm, (132.08 ± 6.22) nm, and (490.13 ± 11.89) nm, respectively. The zeta potential of the three PS MPs/NPs was (-17.90 ± 0.42) mV, (-16.70 ± 1.41) mV and (-17.75 ± 0.92) mV, respectively. The photoluminescence (PL) spectra and UV–vis spectra were shown in [Figure S1](#). The emission peak of the three PS MPs/NPs was about 660–680 nm following excitation at 580 nm, and there was also a UV absorption peak at 650 nm.

Biodistribution of PS MPs/NPs in Mice

After PS MPs/NP was administered into mice by gavage, its biodistribution might be affected by particle size. In order to compare the distribution of PS MPs/NPs with different sizes in mice, cryosection fluorescence microscopy was used and the representative fluorescence images of main tissues from mice treated with 10 mg/kg BW or 1 mg/kg BW PS50, PS100 and PS500 at 28 days are shown in [Figures 2 and 3](#), respectively. The bright and uniform red fluorescence from three types of PS particles could be observed in almost all intestinal and splenic sections and showed a significant dose-dependent effect. The three sizes of PS particles could also be observed in liver and heart tissue sections, but their intensity was weaker than that in the intestine and spleen. Only PS50 could be observed in renal and testicular tissue sections, while three types of PS MPs/NPs could not be observed in brain and lung tissues. It indicated that PS50, PS100 and PS500 could pass through the intestinal barrier and were transported to organs throughout the body with blood. Three different sizes of PS particles were mainly accumulated in the intestine, spleen, liver, and heart, while the smaller particles, PS50 could be distributed in deeper tissues such as testis and kidney.

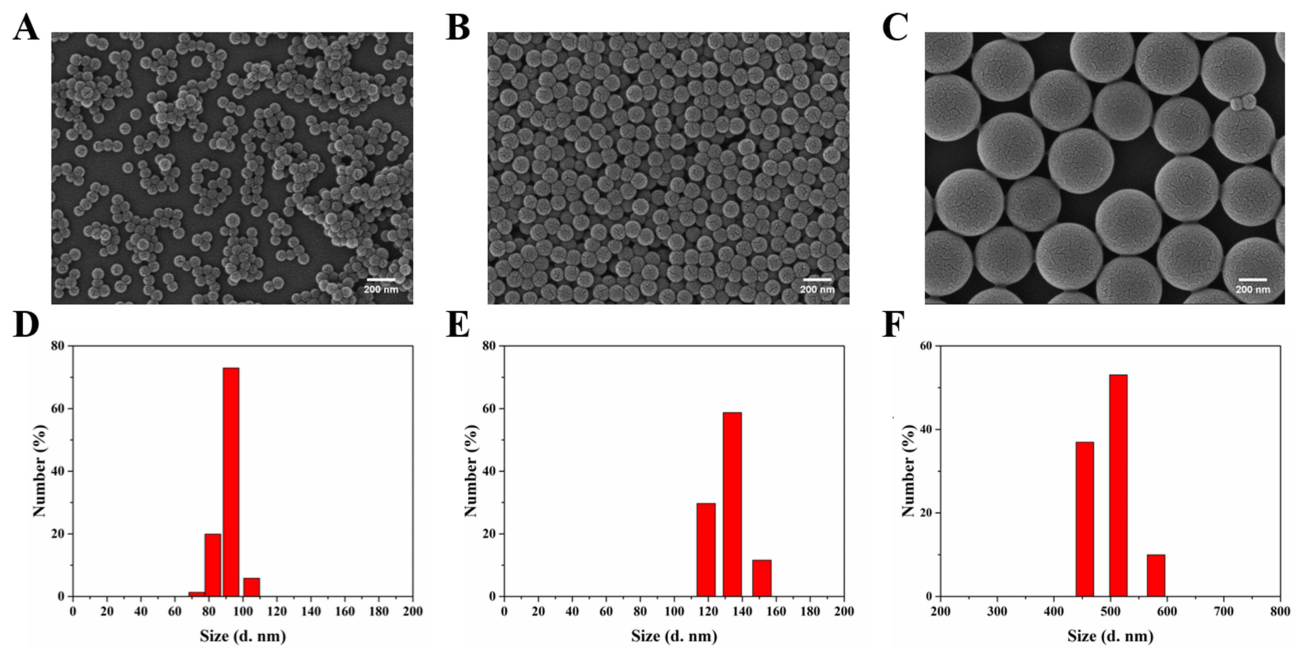


Figure 1 Characterization of three PS MPs/NPs with different sizes. (A–C) SEM image of PS50, PS100, and PS500, respectively (scale bar: 200 nm). (D–F) The hydrodynamic diameter of PS50, PS100, and PS500 dispersed in deionized water.

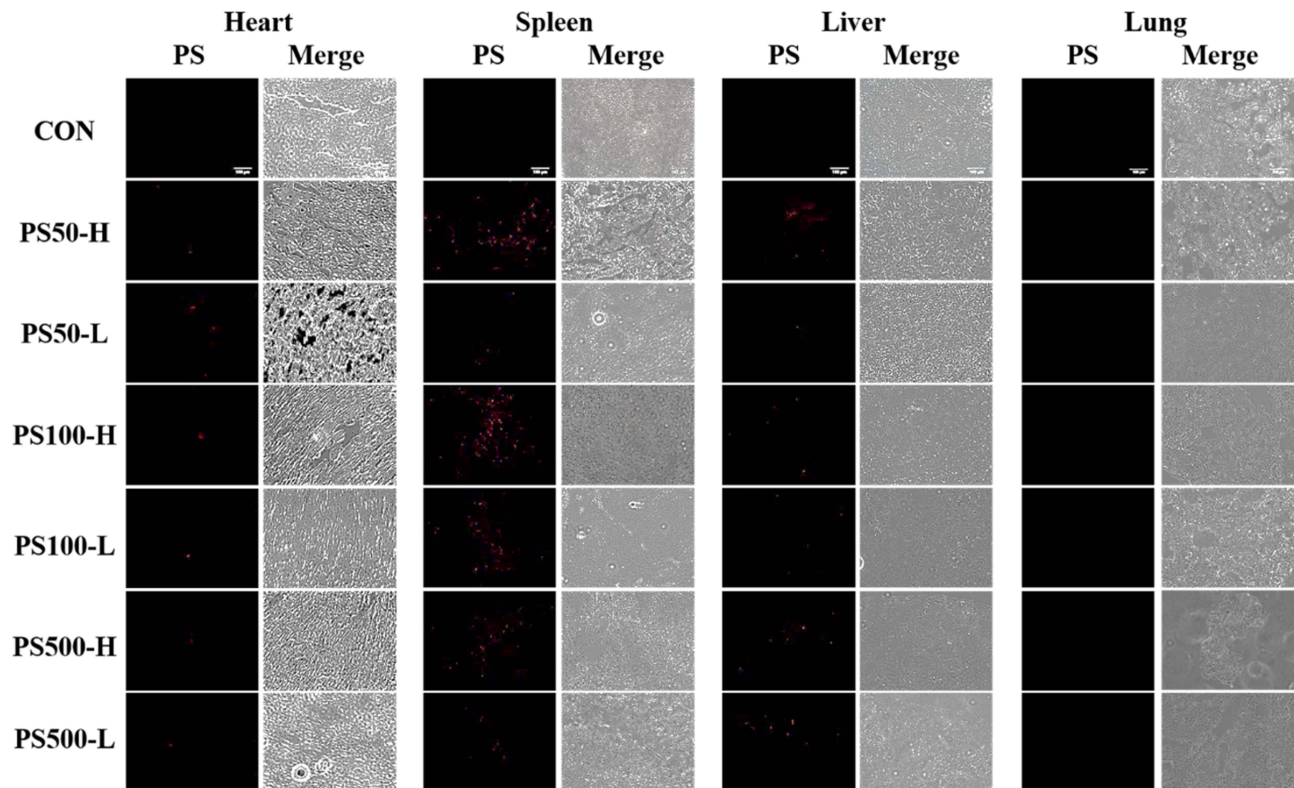


Figure 2 Fluorescence images of heart, spleen, liver and lung tissues after treated with different sizes of PS MPs/NPs (scale bar: 100 μ m).

In order to accurately quantify the accumulation of the three PS MPs/NPs in the main organs with obvious fluorescent signals, the fluorescence intensity of tissue and organ homogenate of mice treated with different particle sizes of PS MPs/NPs was measured by microplate reader. The results were shown in Figure 4A–E. Compared with the control group, the

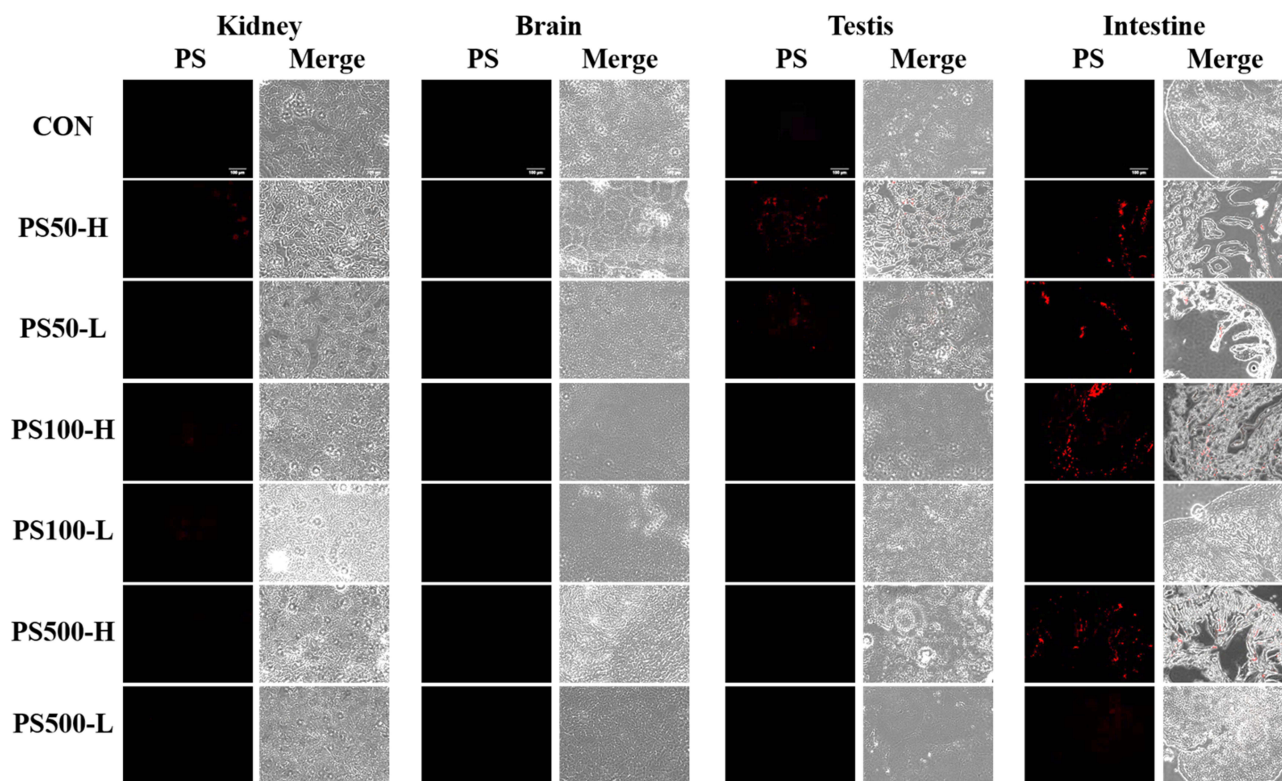


Figure 3 Fluorescence images of kidney, brain, testis and intestine tissues after treated with different sizes of PS MPs/NPs (scale bar: 100 μ m).

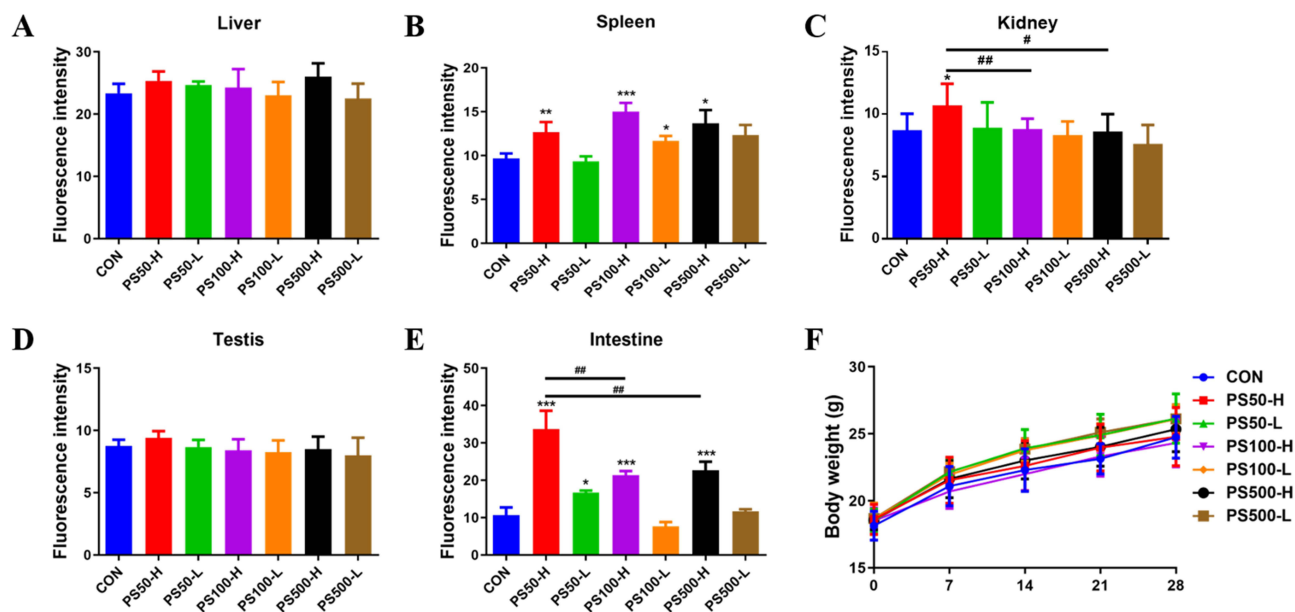


Figure 4 The main tissue fluorescence intensity and body weight of mice after treated with different sizes of PS MPs/NPs for 28 days. **(A)** Fluorescence intensity of liver tissue. **(B)** Fluorescence intensity of spleen tissue. **(C)** Fluorescence intensity of renal tissue. **(D)** Fluorescence intensity of testicular tissue. **(E)** Fluorescence intensity of intestinal tissue. **(F)** The body weight curve of mice continuously monitored for 28 days. **Notes:** * $P < 0.05$, ** $P < 0.01$ and *** $P < 0.001$, Significantly different compared to control group. # $P < 0.05$, ## $P < 0.01$, Significant differences among the treatment groups with different particle sizes at the same exposure dose.

fluorescence intensity of the high-dose group treated with three different sizes of PS MPs/NPs in the intestinal and spleen tissues was significantly increased, and the fluorescence results were consistent with the frozen section. In addition, the fluorescence intensity of kidney tissue in the high-dose group treated with PS50 was significantly higher than that in the

high-dose groups treated with PS100 and PS500. Overall, the fluorescence intensity detection results of tissue homogenate were basically consistent with the trend of image changes in frozen section fluorescence microscopy.

Body Weight and Organ Coefficient

After intragastric administration of PS MPs/NPs once a day, the behavior, food intake, feces and urine of mice were observed and recorded. No mice died throughout the entire experiment. No remarkable changes were observed in behavior, mental status, food intake, and fur after exposure of PS MPs/NPs. The body weight of mice was constantly recorded for 28 days and the statistics are shown in Figure 4F. No significant difference was observed in the growth trend of body weight among different PS treated groups and the control group. The mice were sacrificed at 28 days, and main organs were collected and weighted. The organ coefficient was calculated as the organ weight divided by body weight, and the data are shown in Figure 5. Only the high-dose treatment groups of PS50, PS100, and PS500 showed significantly higher intestinal organ coefficient than that in the low-dose group and control group. No significant statistical differences were observed in other organ coefficients, including the heart, liver, spleen, lung, kidney, brain, and testis among different PS treated groups and the control group. These results indicated that though the three sizes of PS MPs/NP may not significantly affect the growth and development of mice, high doses of PS may have adverse effects on the intestine of mice.

Histopathological Examination Results After PS MPs/NPs Treatment

Although the three sizes of PS MPs/NPs did not have a significant effect on the weight of mice, they could accumulate in the main organs after 28 days of exposure. Histopathological evaluation was performed to evaluate the tissue damage caused by PS MPs/NPs exposure. The representative histological results are shown in Figures 6 and S2. Compared with the control group, in the heart tissue, the high-dose group treated with PS50 showed small areas of calcified lesion in the epicardium (blue arrow), connective tissue proliferation with a small amount of lymphocyte infiltration (black arrow) and the high-dose group treated with PS100 also showed a small amount of lymphocyte infiltration (black arrow). Hepatocyte edema degeneration (black arrow) and hepatocyte steatosis (blue arrow) were observed in the liver tissue of the high-dose group treated with PS50. Mild hydronephrosis of renal tubular epithelial cells could be observed in the renal tissue of the high-dose groups treated with PS50 and PS100 (black arrow). No significant histopathological changes were observed in the main organs of all low-dose PS50, PS100, and PS500 groups, as well as high-dose PS500 groups. The above results indicated that high-dose PS50 caused the most relevant histopathological damage in mice, followed by PS100, and PS500 exhibited almost no significant damage.

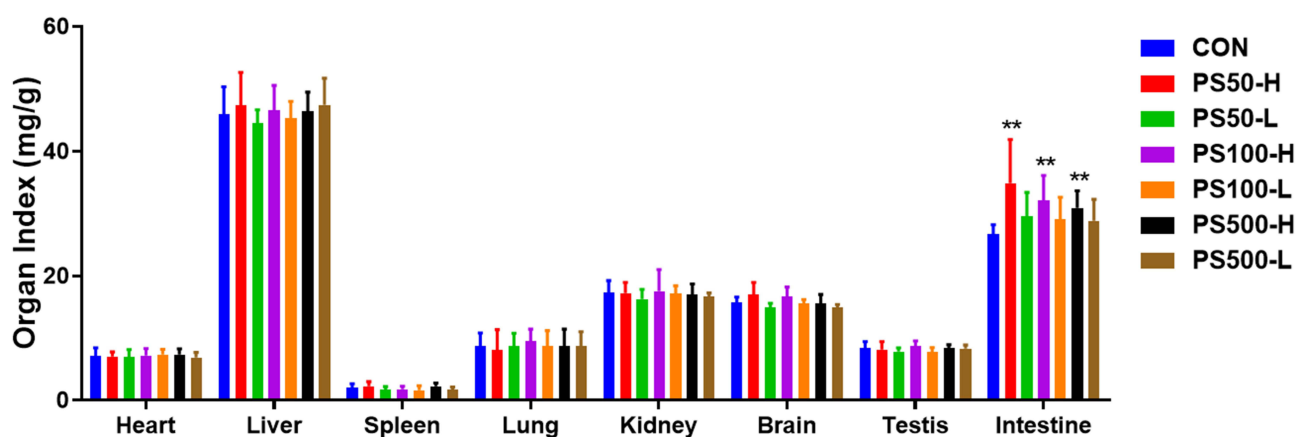


Figure 5 The main organ coefficients of mice after treated with different sizes of PS MPs/NPs for 28 days.
Note: ** $P < 0.01$, significantly different compared to control group.

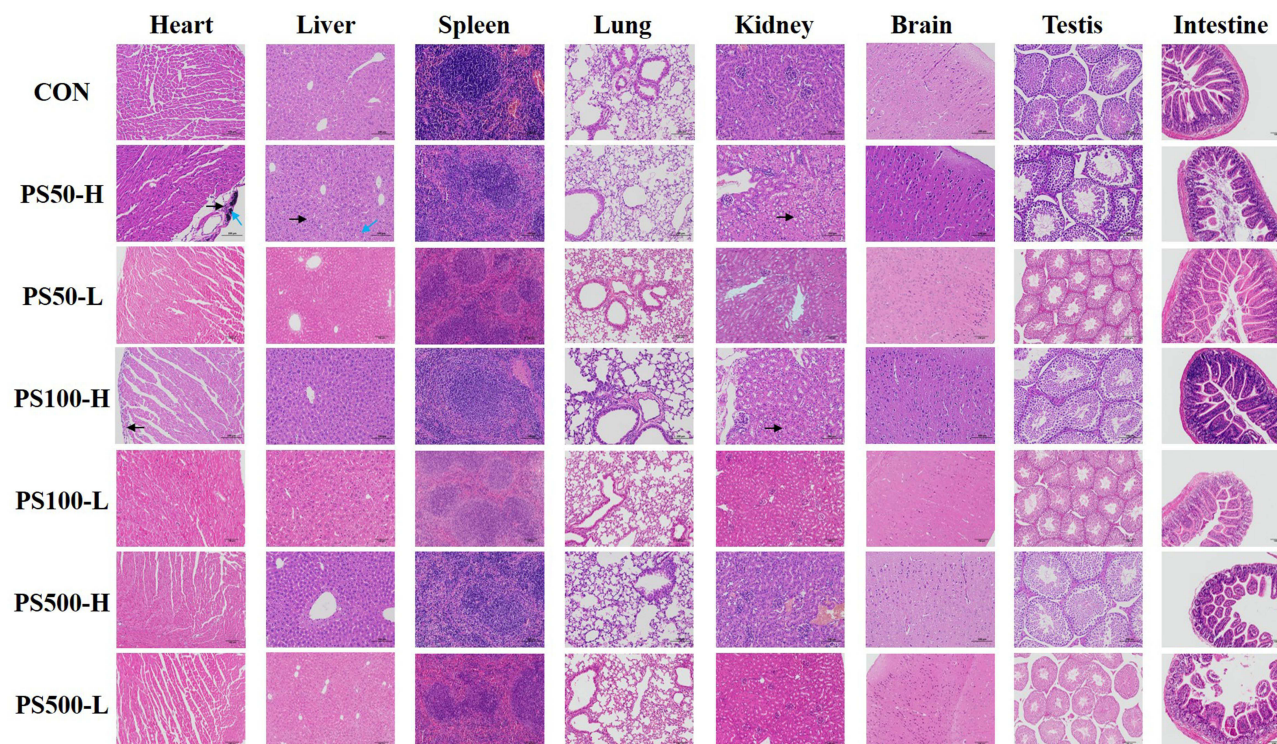


Figure 6 Representative histological images of major organs including heart, liver, spleen, lung, kidney, brain, testis and intestine tissues after treated with different sizes of PS MPs/NPs (scale bar: 100 μ m).

Hematology Analysis After PS MPs/NPs Treatment

Since the three PS MPs/NPs will remain in vivo for a long time, the changes of blood cells could reflect some pathological reactions induced by PS MPs/NPs. Blood routine test was conducted and the results are shown in Figure 7. Compared with the control group, the WBC, Neu counts, and Lym counts of mice both in high-dose and low-dose PS100 treatment groups were significantly reduced after 28 days of gavage. The levels of HGB and MCH in high-dose PS50 group were significantly higher than those in other groups. The PLT levels in PS50-H and PS100-H groups and the PCT levels in the three high-dose groups were remarkably lower than those in control group ($P < 0.05$). No significant differences were found in the other parameters. The above results indicated that high-dose PS of three sizes could cause damage to platelet hematological indicators. In addition, PS100 might cause damage to the immune system in the body, and high dose of PS50 had adverse effects on hemoglobin.

Serum Biochemical Analysis After PS MPs/NPs Treatment

Serum biochemistry tests were performed to observe the effects of different sizes of PS MPs/NPs on the biological functions of major organs, and results are presented in Figure 8. Among the liver-related indicators, levels of TP, ALB, TC and HDL-C in both high-dose PS50 and PS100 treated-groups were significantly lower than those in the control group, while only TP and ALB levels decreased in the high-dose PS500 treatment group when compared with the control group. Additionally, low doses of PS50 and PS100 also lead to a decrease in TP, TC, and HDL-C levels, but no significant changes were observed in all blood biochemical parameters in the low-dose PS500 group. There were no significant differences in ALT, AST, ALP, GLB, TG and LDL-C levels among all PS-treated groups and the control group. Heart function indexes including CK and LDH of all mice were measured and the results are shown in Figure 8L and M. CK levels were significantly increased in the high-dose groups treated with three different sizes of PS MPs/NPs, while LDH levels were only significantly increased in the high-dose groups treated with PS50 and PS100. Meanwhile, low-dose PS50 treatment could also lead to an increase in serum CK levels in mice when compared with the control group. Furthermore, kidney function indexes including UA, UREA and CREA of all mice were also detected, and the

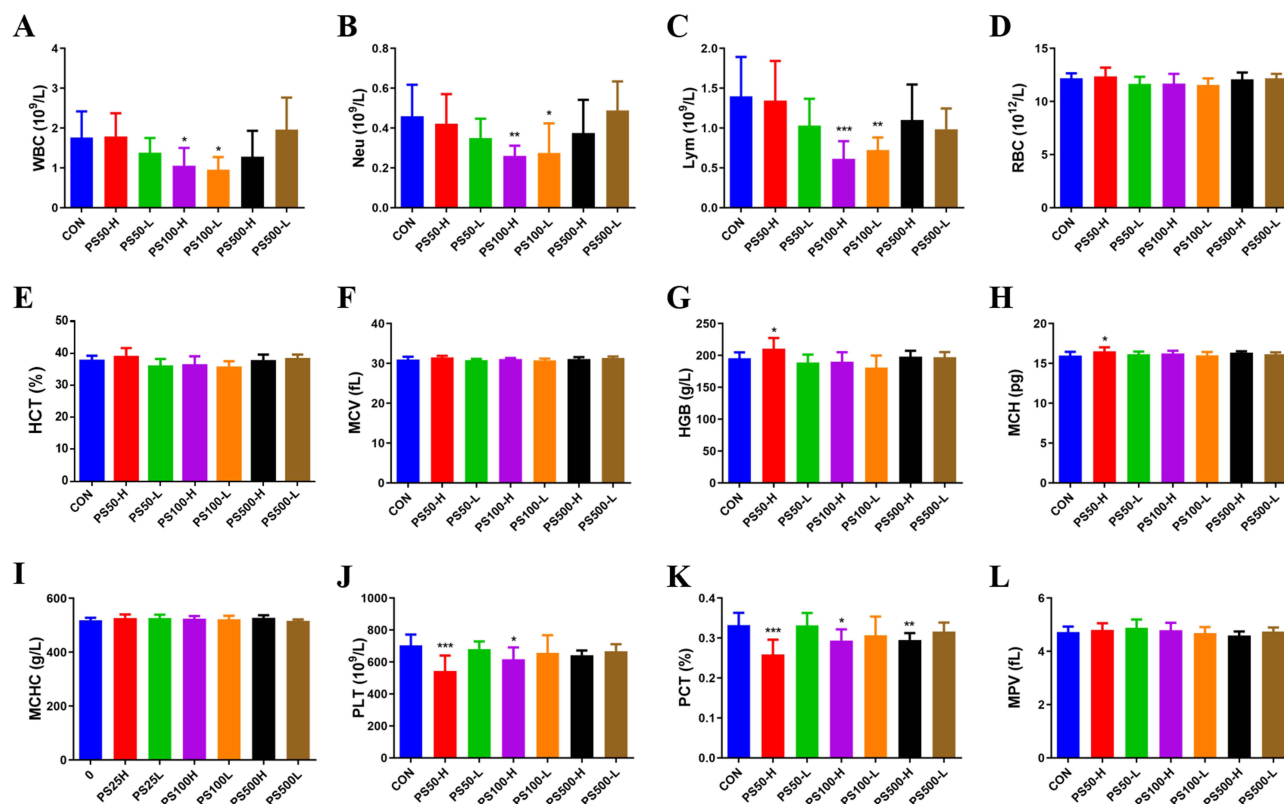


Figure 7 Hematological results of mice after treated with different sizes of PS MPs/NPs. (A) White blood cells (WBC) counts. (B) Neutrophils (NEU) counts. (C) Lymphocytes (Lym) counts. (D) Red blood cell (RBC) counts. (E) Hematocrit (HCT) levels. (F) Mean corpuscular volume (MCV) levels. (G) Hemoglobin concentration (HGB) levels. (H) Mean corpuscular hemoglobin (MCH) levels. (I) Mean corpuscular hemoglobin concentration (MCHC). (J) Platelet (PLT) counts. (K) Thrombopoietin (PCT) levels. (L) Mean platelet volume (MPV) levels. Results were presented as means \pm SD. Statistical analysis was done by one way ANOVA. **Note:** * $P < 0.05$, ** $P < 0.01$ and *** $P < 0.001$, significantly different compared to control group.

results were shown in Figure 8N–P. CREA levels were significantly increased in the high-dose groups treated with three different sizes of PS MPs/NPs, while UREA levels were only significantly increased in the high-dose groups treated with PS50. Three low-dose PS MPs/NPs with different sizes also did not have a significant impact on renal function indicators. The above results indicated that the three sizes of PS MPs/NPs could cause varying degrees of damage in liver, kidney, and heart functions of mice, and there were size- and dose-dependencies. With the size decreased or the dosage increased, the toxicity of PS MPs/NPs to mice increased.

Discussion

Plastic may be degraded into MPs in diameter, and further into NPs in diameter. NPs have been detected in air, soil, water and sludge.³² Research has shown that PS MPs/NPs could enter the human body directly or through the food chain. In the aquatic food chain, MPs and NPs undergo bioaccumulation after being ingested by organisms such as fish and marine mammals and will also be transported through the nutritional level.^{33,34} Therefore, it is very important to understand the accumulation and toxicity of MPs/NPs for human health. Up to now, there are few studies on the toxicity and distribution of PS MPs/NPs, and these studies have basically been carried out by simple model organisms (zebrafish or turbellarian worm) or cell lines in vitro. The mammalian model is the most ideal model for systematically evaluating the toxicity and distribution of exogenous chemicals, as their biological structures are very close to those of humans. Therefore, BALB/c mice were used in this study to evaluate the biodistribution and toxicity of PS MPs/NPs, and the impact of particle size on toxicity was thoroughly and comprehensively studied.

It is well known that the toxicity of exogenous chemicals in vivo is related to many factors, such as dosage, exposure time, route of administration, immune clearance ability of the body. For micro and nanomaterials, the chemical physical properties such as particle size, surface charge, material composition, surface modification, and hydrophilicity largely

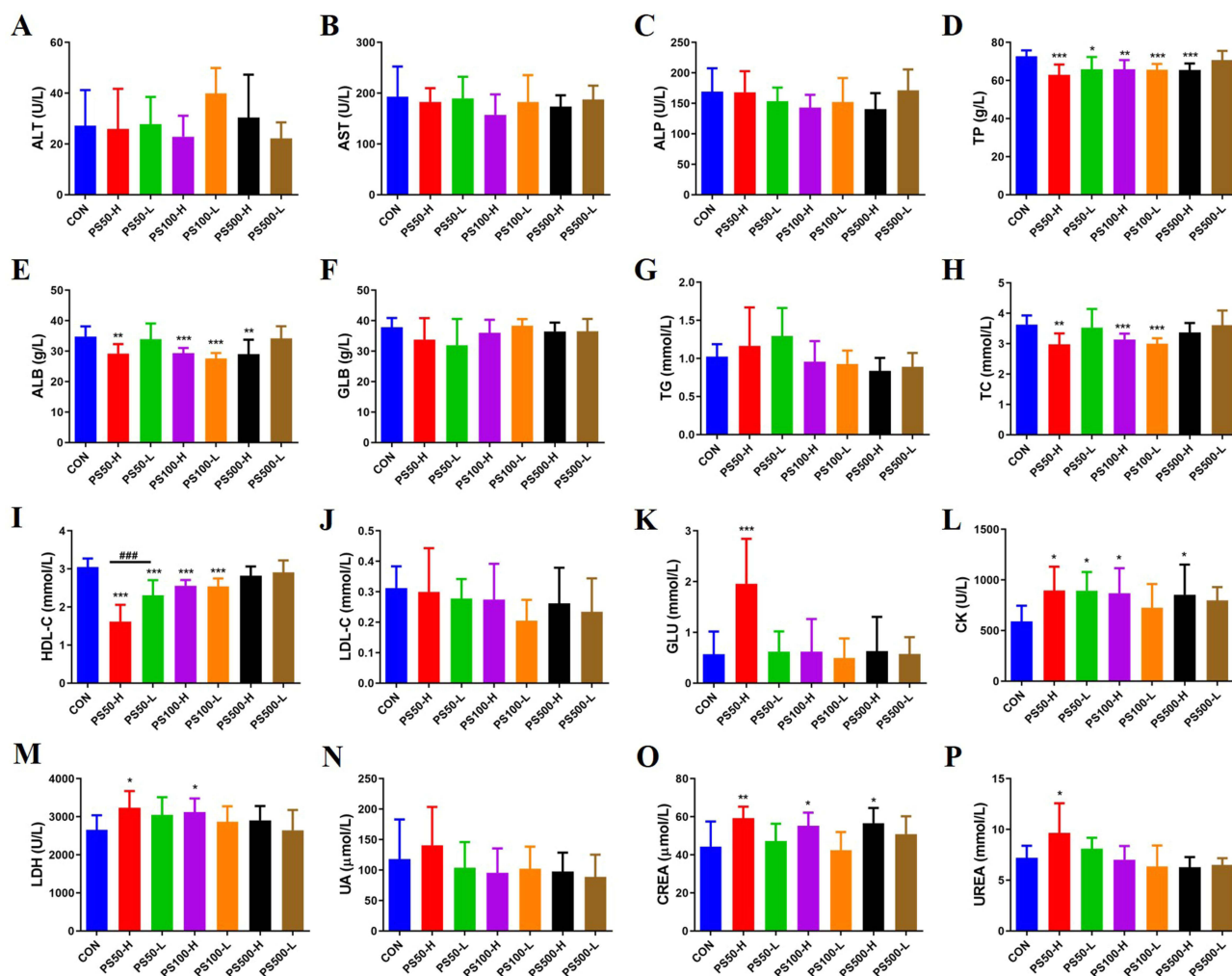


Figure 8 Serum biochemical results of three particle sizes of PS in mice after intragastric administration for 28 days. (A) Alanine aminotransferase (ALT) levels. (B) Aspartate transaminase (AST) levels. (C) Alkaline phosphatase (ALP) levels. (D) Total protein (TP) levels. (E) Albumin (ALB) levels. (F) Globulin (GLB) levels. (G) Triglyceride (TG) levels. (H) Total cholesterol (TC) levels. (I) High-density lipoprotein (HDL-C) levels. (J) Low-density lipoprotein (LDL-C) levels. (K) Glucose (GLU) levels. (L) Creatine kinase (CK) levels. (M) Lactate dehydrogenase (LDH) levels. (N) Uric acid (UA) levels. (O) Creatinine (CREA) levels. (P) Urea levels. **Notes:** * $P < 0.05$, ** $P < 0.01$ and *** $P < 0.001$, significantly different compared to control group. #### $P < 0.001$, significant differences among the treatment groups with different particle sizes at the same exposure dose.

determine their biodistribution and toxicity.^{35–37} Among them, particle size is one of the most effective factors affecting the biodistribution and toxicity.³⁵ In order to reveal the difference between the effects of NPs and MPs on human health, the accumulation and toxicity of PS with different particle sizes in various organs and tissues of mice were analyzed after 28 days of continuous exposure. Previous studies have shown that MPs can accumulate in the intestine, and the digestive tract is also considered to be the main exposure route of PS MPs/NPs.³⁸ Therefore, we established the method of intragastric administration to construct the mouse model after PS MPs/NPs exposure. According to relevant literature reports, the mean of the sum quantifiable concentration of plastic particles in blood was 1.6 $\mu\text{g}/\text{mL}$.¹⁰ As the total blood volume of a 70 kg healthy adult is about 4900 mL, the total plastic particles is 7840 μg by calculation, and the actual human exposure is about 0.112 mg/kg body weight. According to the biological safety factors of different species, the exposure doses of 1 mg/kg and 10 mg/kg were selected in this study, which were 10 times and 100 times higher than the human exposure dose. Based on plastic particles exposed to humans daily and the accumulation in the body, the exposure dose was determined in the present study. The tissue biodistribution and toxicity in different organs of PS MPs/NPs with different sizes (50 nm, 100 nm, 500 nm) and doses (10 mg/kg BW, 1 mg/kg BW) were systematically studied in BALB/c

mice after intragastric administration for 28 days, which help us make up for the lack of toxicity study of PS MPs/NPs in mammals.

The biodistribution and accumulation of PS MPs/NPs are the key parameters to evaluate their toxicity *in vivo*.²⁸ Several studies have reported that the biodistribution of PS MPs/NPs in animal models is significantly dependent on particle size. Lu et al reported that 5 μm diameter PS-MPs accumulated in fish gills, liver, and gut after 7 days of exposure, while larger-sized 20 μm diameter PS-MPs accumulated only in fish gills and gut and no particles were found in liver.³⁹ Torres-Ruiz et al demonstrated that NP accumulation depended on the particle size. Smaller NP could reach internal organs (brain, eyes, liver, pancreas, heart) but larger (>200 nm) accumulated mainly in gut, gills and skin.⁴⁰ Zitouni et al reported that the concentration of particles $\geq 3 \mu\text{m}$ was higher in the gills, while particles ranging from 3 to 0.45 μm were most likely to be accumulated in the guts and livers, and there were significant differences in the tissue distribution of particles with different sizes.⁴¹ In this study, cryosection fluorescence microscopy and microplate reader were utilized to detect the distribution of the three sizes of PS MPs/NPs in mice after intragastric administration for 28 days. Bright and uniform red fluorescence from three sizes of PS MPs/NPs could be observed in the frozen sections of most organs, and the fluorescence intensity of intestinal tract was the highest. Furthermore, the fluorescence intensity of organs in PS50 and PS100 treated-groups was higher than that in PS500 treated-group. The results showed that the three sizes of PS MPs/NPs first entered the digestive tract through gastrointestinal tissue and then distributed in the heart, liver, spleen, kidney and intestine with blood circulation. Among them, PS50 and PS100 groups were more widely distributed and accumulated. In order to avoid the interference of environmental factors and tissue self-fluorescence on the fluorescence signal of frozen sections, the fluorescence intensity of PS in the homogenate of five organs (liver, spleen, kidney, brain, and intestine) was measured by a fluorescence reader, and the results were basically consistent with the fluorescence images of the tissues. In the experiment, we also found that the fluorescence intensity was detected in the lysate and organ tissue background, which would bring some interference to the experiment. However, due to the same organ and tissue quality and test conditions, the control group can also be used as a standard reference. This indicated that the distribution of plastic particles in the body had a significant particle size dependence, and compared to MPs, NPs with smaller particle sizes were more likely to penetrate biological barriers and distribute in major organs.

As the three sizes of PS MPs/NPs could accumulate in the main organs of mice from the results of fluorescence imaging, more attention should be paid to the biological toxicity caused by their distribution and accumulation. In the present study, histopathological examination, hematology, and serum biochemical analysis were performed. Although the growth, mental state, and weight of the mice did not change after 28 days of exposure to different sizes of PS MPs/NPs, the high-dose groups of three particle sizes could increase the intestinal organ coefficient in mice. HE et al observed a decrease in duodenal villus length and crypt depth in mice treated with 102 nm of PS NPs.⁴² Therefore, the increase of the intestinal organ coefficient may be due to intestinal permeability leading to intestinal cell hydronephrosis. However, no obvious intestinal cell damage was observed by H&E staining, indicating that PS MPs/NPs had limited effect on intestinal injury.

According to the analysis of hematological results, the WBC counts of the high-dose and low-dose groups treated with PS100 were significantly reduced. It has been reported that lower WBC is usually associated with a weak immune system in human beings.⁴³ PS100 may cause damage to the immune system of mice. Platelet-related indexes (PLT, PCT) in PS50 and PS100 groups were significantly decreased, indicating that nanoplastics may cause coagulation dysfunction. Furthermore, it was found that HGB and MCHC increased significantly in PS50-H group, changes to erythrocyte content, hematocrit values, and hemoglobin concentrations reflect the defense mechanisms to stress caused by exposure to environmental toxicity. The relative increase of hemoglobin may also be due to the loss of water in plasma and the concentration of blood, resulting in the relative increase of red blood cells and hemoglobin.⁴⁴

Zhu et al unveils that cardiac toxicity of PS MPs/NPs included abnormal heart rate, cardiac function impairment, pericardial edema, and myocardial fibrosis. Cardiovascular toxicity was determined by the properties (type, size, surface, and structure) of MPs/NPs, exposure dose and duration.⁴⁵ Lu et al found that zebrafish hepatocytes in MP treatment group had early inflammatory reactions, such as vacuolation, infiltration and necrosis.⁴⁶ However, due to the different species and exposed particle sizes, the nanoplastics represented by PS50 and PS100 in this study will cause pathological damage to the liver. Although many hepatotoxicity studies have shown that the liver may be the main target organ of nanomaterials, the difference of liver injury in mice caused by the three particle sizes has not been reported before. Tang et al found that PS NPs

caused tubular lumen narrowing, tubular epithelial cell detachment and vacuolar degeneration.⁴⁷ In this study, PS50 may penetrate the renal tissue and cause pathological damage to the kidney. In the blood biochemical indicators, the accumulation of three sizes of PS MPs/NPs in tissues will lead to liver function damage. The increase of AST, ALT and LDH levels and the decrease of ALB levels can reflect the damage of hepatocytes and liver function. In addition, the decrease of TC and HDL-C after PS50 and PS100 treated-groups indicated that PS NPs exposure induced lipid metabolism disorder. In addition, the decrease of TC and HDL-C after PS50 and PS100 treatment groups indicated that PS NPs exposure induced lipid metabolism disorder. Meanwhile, representative H&E image of liver also showed steatosis of liver cells. Hepatocyte steatosis is a phenotype often observed under inflammatory conditions and is used as the index of inflammatory response.⁴⁸ As a result, NP exposure may cause inflammatory response, which leading to liver lipid disorder. Glucose levels are maintained through homeostasis, by balancing glucose production with the storage of glucose as glycogen.⁴⁹ In PS50-H treated-group, there is a significant increase in GLU, and it is likely that the fatty degeneration of liver cells causes glucose metabolism disorder.⁵⁰ In this study, exposure to high-dose PS resulted in slightly increased cardiac injury index CK and LDH. Previous studies have also demonstrated that PS MPs/NPs affected cardiac functions and caused toxicity on (micro)vascular sites. In addition, histopathological analysis also showed that the heart structure of PS50-H and PS100-H treated-groups was slightly damaged. Exposure to high doses of PS with three particle sizes can cause kidney damage in mice. The increase of creatinine and urea levels showed that the renal function was impaired.⁵¹ Mild hydronephrosis of renal tubular epithelial cells was also observed in the renal histological images of PS50-H and PS100-H treated-groups. These results indicated that PS MPs/NPs exposure is likely to cause decrease in kidney function.

In this study, BALB/c mice were gavage with the three sizes of PS MPs/NPs for 28 days. The results indicated that three different sizes of PS could be distributed in the main organs of mice and lead to mild changes in biochemical indicators and pathological damage of liver, kidney, and heart function. No significant toxicological changes were observed in this study. This may be due to the 28 days exposure period was not be long enough. It may be necessary to choose longer exposure time to evaluate the potential toxicity and damage of plastics to the body. In conclusion, the size of PS MPs/NPs is an important factor affecting the accumulation and biological toxicity in mice.

Conclusion

In this study, the biodistribution and toxicity of PS MPs/NPs with different particle sizes in BALB/c mice were evaluated systematically. PS MPs/NPs with three particle sizes could accumulate in main tissues and organs of mice. At the same time, the smaller the particle size, the more it accumulates in the body and the wider its distribution. In addition, PS NPs can cause more obvious pathological changes in the heart, liver and kidney of mice than PS MPs, and affect the serum biochemical indexes related to these organs. In conclusion, this study shows that different particle sizes of PS cause different distribution and toxicity in mice, which helps to pay more attention to the potential adverse effects of nanoplastics on human health.

Funding

This study was funded by the National Natural Science Foundation of China (NSFC) (Grant 82373615 and 82103891), Discipline Construction “Clinical+Basic” Special Project of Guangdong Medical University (4SG24006G), and Provincial College Student Innovation and Entrepreneurship Training Program Project (Grant No. S202310571111).

Disclosure

The authors report no conflicts of interest in this work.

References

1. Kim J, Maruthupandy M, S AK, et al. Acute and subacute repeated oral toxicity study of fragmented microplastics in Sprague-Dawley rats. *Ecotoxicol Environ Saf*. 2021;228:112964. doi:10.1016/j.ecoenv.2021.112964
2. Galloway TS, Cole M, Lewis C. Interactions of microplastic debris throughout the marine ecosystem. *Nat Ecol Evol*. 2017;1(5):116. doi:10.1038/s41559-017-0116
3. Wei J, Wang X, Liu Q, et al. The impact of polystyrene microplastics on cardiomyocytes pyroptosis through NLRP3/Caspase-1 signaling pathway and oxidative stress in Wistar rats. *Environ Toxicol* 2021;36(5):935–944. doi:10.1002/tox.23095

4. Li L, Xu M, He C, et al. Polystyrene nanoplastics potentiate the development of hepatic fibrosis in high fat diet fed mice. *Environ Toxicol.* 2022;37(2):362–372. doi:10.1002/tox.23404
5. Zhang Y, Gao T, Kang S, et al. Importance of atmospheric transport for microplastics deposited in remote areas. *Environ Pollut.* 2019;254(Pt A):112953. doi:10.1016/j.envpol.2019.07.121
6. Barria C, Brandts I, Tort L, et al. Effect of nanoplastics on fish health and performance: a review. *Mar Pollut Bull.* 2020;151:110791. doi:10.1016/j.marpolbul.2019.110791
7. Sun H, Jiao R, Wang D. The difference of aggregation mechanism between microplastics and nanoplastics: role of Brownian motion and structural layer force. *Enviro poll.* 2021;268(Pt B):115942. doi:10.1016/j.envpol.2020.115942
8. Schwabl P, Köppel S, Königshofer P, et al. Detection of various microplastics in human stool: A prospective case series. *Ann Intern Med.* 2019;171(7):453–457. doi:10.7326/m19-0618
9. Ragusa A, Svelato A, Santacroce C, et al. Plasticenta: First evidence of microplastics in human placenta. *Environ Int.* 2021;146:106274. doi:10.1016/j.envint.2020.106274
10. Leslie HA, van Velzen MJM, Brandsma SH, et al. Discovery and quantification of plastic particle pollution in human blood. *Environ Int.* 2022;163:107199. doi:10.1016/j.envint.2022.107199
11. Wang L, Wu WM, Bolan NS, et al. Environmental fate, toxicity and risk management strategies of nanoplastics in the environment: Current status and future perspectives. *J Hazard Mater.* 2021;401:123415. doi:10.1016/j.jhazmat.2020.123415
12. Carr KE, Smyth SH, McCullough MT, et al. Morphological aspects of interactions between microparticles and mammalian cells: intestinal uptake and onward movement. *Prog Histochem Cytochem.* 2012;46(4):185–252. doi:10.1016/j.proghi.2011.11.001
13. Yan Z, Liu Y, Zhang T, et al. Analysis of microplastics in human feces reveals a correlation between fecal microplastics and inflammatory bowel disease status. *Environ Sci Technol.* 2022;56(1):414–421. doi:10.1021/acs.est.1c03924
14. Liu L, Xu K, Zhang B, et al. Cellular internalization and release of polystyrene microplastics and nanoplastics. *Sci Total Environ.* 2021;779:146523. doi:10.1016/j.scitotenv.2021.146523
15. Hirt N, Body-Malapel M. Immunotoxicity and intestinal effects of nano- and microplastics: a review of the literature. *Part Fibre Toxicol.* 2020;17(1):57. doi:10.1186/s12989-020-00387-7
16. Song YK, Hong SH, Eo S, et al. Rapid production of micro- and nanoplastics by fragmentation of expanded polystyrene exposed to sunlight. *Environ Sci Technol.* 2020;54(18):11191–11200. doi:10.1021/acs.est.0c02288
17. Kopatz V, Wen K, Kovacs T, et al. Micro- and nanoplastics breach the blood-brain barrier (bbb): biomolecular corona's role revealed. *Nanomaterials (Basel).* 2023;13(8):1404. doi:10.3390/nano13081404
18. Stock V, Böhmert L, Lisicki E, et al. Uptake and effects of orally ingested polystyrene microplastic particles in vitro and in vivo. *Arch Toxicol.* 2019;93(7):1817–1833. doi:10.1007/s00204-019-02478-7
19. Zhou N, Wang Z, Yang L, et al. Size-dependent toxicological effects of polystyrene microplastics in the shrimp *Litopenaeus vannamei* using a histomorphology, microbiome, and metabolic approach. *Environ Pollut.* 2023;316(Pt 2):120635. doi:10.1016/j.envpol.2022.120635
20. Jung BK, Han SW, Park SH, et al. Neurotoxic potential of polystyrene nanoplastics in primary cells originating from mouse brain. *Neurotoxicology.* 2020;81:189–196. doi:10.1016/j.neuro.2020.10.008
21. Hussain N, Jaitley V, Florence AT. Recent advances in the understanding of uptake of microparticulates across the gastrointestinal lymphatics. *Adv Drug Deliv Rev.* 2001;50(1–2):107–142. doi:10.1016/s0169-409x(01)00152-1
22. Yoo JW, Doshi N, Mitragotri S. Adaptive micro and nanoparticles: temporal control over carrier properties to facilitate drug delivery. *Adv Drug Deliv Rev.* 2011;63(14–15):1247–1256. doi:10.1016/j.addr.2011.05.004
23. Li L, Chen T, Yang Z, et al. Nephrotoxicity evaluation of indium phosphide quantum dots with different surface modifications in BALB/c Mice. *Int J Mol Sci.* 2020;21(19):7137. doi:10.3390/ijms21197137
24. Choi CH, Zuckerman JE, Webster P, et al. Targeting kidney mesangium by nanoparticles of defined size. *Proc Natl Acad Sci U S A.* 2011;108(16):6656–6661. doi:10.1073/pnas.1103573108
25. Simon BH, Ando HY, Gupta PK. Circulation time and body distribution of 14C-labeled amino-modified polystyrene nanoparticles in mice. *J Pharmaceut Sci.* 1995;84(10):1249–1253. doi:10.1002/jps.2600841020
26. Xu D, Ma Y, Han X, et al. Systematic toxicity evaluation of polystyrene nanoplastics on mice and molecular mechanism investigation about their internalization into Caco-2 cells. *J Hazard Mater.* 2021;417:126092. doi:10.1016/j.jhazmat.2021.126092
27. Liang B, Zhong Y, Huang Y, et al. Underestimated health risks: polystyrene micro- and nanoplastics jointly induce intestinal barrier dysfunction by ROS-mediated epithelial cell apoptosis. *Part Fibre Toxicol.* 2021;18(1):20. doi:10.1186/s12989-021-00414-1
28. Deng Y, Zhang Y, Lemos B, et al. Tissue accumulation of microplastics in mice and biomarker responses suggest widespread health risks of exposure. *Sci Rep.* 2017;7:46687. doi:10.1038/srep46687
29. Gao T, Sun B, Xu Z, et al. Exposure to polystyrene microplastics reduces regeneration and growth in planarians. *J Hazard Mater.* 2022;432:128673. doi:10.1016/j.jhazmat.2022.128673
30. Pitt JA, S KJ, Jayasundara N, et al. Uptake, tissue distribution, and toxicity of polystyrene nanoparticles in developing zebrafish (*Danio rerio*). *Aquat Toxicol.* 2018;194:185–194. doi:10.1016/j.aquatox.2017.11.017
31. Greven AC, Merk T, Karagoz F, et al. Polycarbonate and polystyrene nanoplastic particles act as stressors to the innate immune system of fathead minnow (*Pimephales promelas*). *Environ Toxicol Chem.* 2016;35(12):3093–3100. doi:10.1002/etc.3501
32. Kik K, Bukowska B, Sicińska P. Polystyrene nanoparticles: Sources, occurrence in the environment, distribution in tissues, accumulation and toxicity to various organisms. *Enviro poll.* 2020;262:114297. doi:10.1016/j.envpol.2020.114297
33. Carbery M, O'Connor W, Palanisami T. Trophic transfer of microplastics and mixed contaminants in the marine food web and implications for human health. *Environ Int.* 2018;115:400–409. doi:10.1016/j.envint.2018.03.007
34. A BLG, R VL, Branco V, et al. Microplastics cause neurotoxicity, oxidative damage and energy-related changes and interact with the bioaccumulation of mercury in the European seabass, *Dicentrarchus labrax* (Linnaeus, 1758). *Aquat Toxicol.* 2018;195:49–57. doi:10.1016/j.aquatox.2017.12.008
35. P WA, Kramer E, J HP, et al. Translocation of differently sized and charged polystyrene nanoparticles in in vitro intestinal cell models of increasing complexity. *Nanotoxicology.* 2015;9(4):453–461. doi:10.3109/17435390.2014.944599
36. Stock V, Laurisch C, Franke J, et al. Uptake and cellular effects of PE, PP, PET and PVC microplastic particles. *Toxicol In Vitro.* 2021;70:105021. doi:10.1016/j.tiv.2020.105021

37. P WA, J HP, A WR, et al. Bioavailability and biodistribution of differently charged polystyrene nanoparticles upon oral exposure in rats. *J Nanopart Res.* 2015;17(5):231. doi:10.1007/s11051-015-3029-y
38. Lu L, Wan Z, Luo T, et al. Polystyrene microplastics induce gut microbiota dysbiosis and hepatic lipid metabolism disorder in mice. *Sci Total Environ.* 2018;631-632:449–458. doi:10.1016/j.scitotenv.2018.03.051
39. Lu Y, Zhang Y, Deng Y, et al. Uptake and accumulation of polystyrene microplastics in zebrafish (danio rerio) and toxic effects in liver. *Environ. Sci. Technol.* 2016;50(7):4054–4060. doi:10.1021/acs.est.6b00183
40. Torres-Ruiz M, De la Vieja A, de Alba Gonzalez M, et al. Toxicity of nanoplastics for zebrafish embryos, what we know and where to go next. *Sci Total Environ.* 2021;797:149125. doi:10.1016/j.scitotenv.2021.149125
41. Zitouni N, Bousserhine N, Missawi O, et al. Uptake, tissue distribution and toxicological effects of environmental microplastics in early juvenile fish *Dicentrarchus labrax*. *J Hazard Mater.* 2021;403:124055. doi:10.1016/j.jhazmat.2020.124055
42. He Y, Li Z, Xu T, et al. Polystyrene nanoplastics deteriorate LPS-modulated duodenal permeability and inflammation in mice via ROS driven-NF- κ B/NLRP3 pathway. *Chemosphere.* 2022;307(Pt 1):135662. doi:10.1016/j.chemosphere.2022.135662
43. Ono M, Tomaniak M, Koenig W, et al. Impact of white blood cell count on clinical outcomes in patients treated with aspirin-free ticagrelor monotherapy after percutaneous coronary intervention: insights from the GLOBAL LEADERS trial. *Eur Heart J Cardiovasc Pharmacother.* 2022;8(1):39–47. doi:10.1093/ehjcvp/pvaa110
44. Iheanacho SC, Odo GE. Neurotoxicity, oxidative stress biomarkers and haematological responses in African catfish (*Clarias gariepinus*) exposed to polyvinyl chloride microparticles. *Comp Biochem Physiol C Toxicol Pharmacol.* 2020;232:108741. doi:10.1016/j.cbpc.2020.108741
45. Zhu X, Wang C, Duan X, et al. Micro- and nanoplastics: a new cardiovascular risk factor? *Environ Int.* 2023;171:107662. doi:10.1016/j.envint.2022.107662
46. Lu Y, Zhang Y, Deng Y, et al. Uptake and accumulation of polystyrene microplastics in zebrafish (danio rerio) and toxic effects in liver. *Environ Sci Technol.* 2016;50(7):4054–4060. doi:10.1016/j.jhazmat.2021.126092
47. Tang Y, Zhao R, Pu Q, et al. Investigation of nephrotoxicity on mice exposed to polystyrene nanoplastics and the potential amelioration effects of DHA-enriched phosphatidylserine. *Sci Total Environ.* 2023;892:164808. doi:10.1016/j.aquatox.2017.12.008
48. Bozza PT. Uptake and Accumulation of Polystyrene Microplastics in Zebrafish (*Danio rerio*) and Toxic Effects in Liver. *Prostaglandins Leukot Essent Fatty Acids.* 2010;82(4–6):164808–164850. doi:10.1016/j.scitotenv.2023.164808
49. B RJF, M LM, E RW, et al. Microplastics and copper effects on the neotropical teleost *Prochilodus lineatus*: is there any interaction? *Comp Biochem Physiol a Mol Integr Physiol.* 2020;242:110659. doi:10.1016/j.cbpa.2020.110659
50. W CH, Chao SW, Lin H, et al. Homeostasis of glucose and lipid in non-alcoholic fatty liver disease. *Int J Mol Sci.* 2019;20(2):298. doi:10.3390/ijms20020298
51. Mu L, Zhu L, Feng Y, et al. Nephropathy 1st inhibits renal fibrosis by activating the PPAR γ signaling pathway. *Front Pharmacol.* 2022;13:992421. doi:10.3389/fphar.2022.992421

International Journal of Nanomedicine

Dovepress

Publish your work in this journal

The International Journal of Nanomedicine is an international, peer-reviewed journal focusing on the application of nanotechnology in diagnostics, therapeutics, and drug delivery systems throughout the biomedical field. This journal is indexed on PubMed Central, MedLine, CAS, SciSearch[®], Current Contents[®]/Clinical Medicine, Journal Citation Reports/Science Edition, EMBase, Scopus and the Elsevier Bibliographic databases. The manuscript management system is completely online and includes a very quick and fair peer-review system, which is all easy to use. Visit <http://www.dovepress.com/testimonials.php> to read real quotes from published authors.

Submit your manuscript here: <https://www.dovepress.com/international-journal-of-nanomedicine-journal>